Dealing with Stochastic Uncertainty and Prediction in Extreme Driving

Siddharth Gangadhar[1†], Zhuoyuan Wang[1†], Haoming Jing[1], and Yorie Nakahira[1]

***Abstract*— In this paper, we use an extreme driving scenario as a case study to present a safe control technique that can adapt to changing environments, tolerate large uncertainties, and exploit predictions in an integrated manner. We first derive a sufficient condition to ensure long-term safe probability when there are uncertainties in system parameters. Then, we use the safety condition to formulate a stochastic safe control technique. Finally, we test the proposed technique numerically in extreme driving scenarios. The use of long-term safe probability provides a sufficient outlook time horizon to capture future predictions of the environment and planned vehicle maneuvers and to avoid unsafe regions of attractions. The resulting control action systematically mediates behaviors based on the level of uncertainties and can find safer actions even with large uncertainties. This feature allows the system to quickly respond to changes and risks, even before an accurate estimate of the changed parameters can be constructed. The safe probability can be continuously learned and refined, and the use of more accurate probability helps avoid over-conservatism, which is a common drawback of a deterministic worst-case approach. The proposed techniques can also be efficiently computed in real-time using onboard hardware and modularly integrated into existing processes such as predictive model controllers.**

I. Introduction

Background. Safe driving in extreme environments (e.g. icy roads with low traction) is challenging for both human drivers and autonomous vehicles. The vehicle parameters can vary by driving conditions, and the control strategy must adapt to changes quickly. These parameters may have large uncertainties before the their changes can be accurately estimated. In adverse conditions, the uncertainties due to unmodeled dynamics and noise in sensing, localization, and estimation can be particularly large. Moreover, the vehicles' states can have unsafe regions of attractions, in which controllability and stability are significantly reduced. The likelihood of entering such regions depends on the future road condition (traction, curvature, etc.), planned maneuvers and actions, predictions of the environments as well as their levels of uncertainties. Therefore, it is critical in extreme driving to adapt to changes, mediate behaviors based on uncertainties, exploit predictions, and do them in an integrated manner.

Related work. Various techniques have been developed for advanced driving assistance systems (ADASs) and autonomous vehicles (AVs). Many of these techniques are developed in deterministic worst-case frameworks: H-infinity controllers [1], robust sliding mode controllers [2], fuzzy logic controllers [3], and control barrier functions [4]. These techniques can often be efficiently computed but require full system models and small bounded uncertainties (errors). In the presence of large uncertainties, these techniques may not perform well: ensuring safety for all possible errors may be infeasible; the performance may not degrade gracefully for increasing uncertainties due to overly conservative actions.

When there are unknown parameters or changes in the internal and external parameters, techniques have been developed for parameter estimation as well as fast adaptation. Some combine parameter estimates (e.g., Kalman filter, Bayesian filter) and additional modifications in control to account for uncertainties [5]. The modification in control techniques is often built on worst-case frameworks and similarly assumes the availability of accurate estimates. Others direct estimate the control parameters using PID tuning [6], interactive learning methods [7]. The performance guarantees (convergence) of these methods often require the system dynamics to take some specific structures, and they often do not exploit future predictions.

Various model predictive control (MPC) techniques have been developed to better exploit future predictions and balance different performance objectives [8]–[10]. These methods look out into future time horizons and use predictions to achieve better performance. As the number of possible trajectories grows exponentially to the outlook time horizon, there are often stringent tradeoffs between outlook time horizon and computation burdens.

To better account for uncertainties, many methods use stochastic frameworks. Examples of these techniques are stochastic MPC [11] and chance-constrained MPC [12]. Control of distributions and constraints of probability can be efficiently computed under certain assumptions such as linear dynamics and Gaussian disturbances. However, for general (nonlinear) systems, there do not exist lightweight algorithms suitable for online or onboard computation. Here too, there exists a severe tradeoff between outlook time horizon and computation load because computing and constraining long-term probability requires characterizing the evolution of complex state distributions over time.

Our contributions. Motivated by these challenges, we propose a stochastic safe control technique that accounts for internal parameter changes, planned vehicle control, and the prediction of environmental factors. The technique efficiently (myopically) finds a control action with ensured long-term safe probability. The method can both flexibly adapt to changes and remain robust in a steady state by mediating behaviors based on the levels of parameter uncertainties. The long-term safe probability can represent a variety of perfor-

†These authors contributed equally.

[1]Siddharth Gangadhar, Zhuoyuan Wang, Haoming Jing, and Yorie Nakahira are with the Department of Electrical and Computer Engineering, Carnegie Mellon Universty, {sgangadh,zhuoyuaw,haomingj,ynakahir}@andrew.cmu.edu.

mance/safety specifications, and its probability measure can be continuously learned based on driving data.

Specifically, we derive a safety condition that ensures the safe probability to stay above a tolerable level. The safety condition is then used to construct a safe control algorithm that can be efficiently computed in real-time and modularly embedded into existing decision-making processes. The algorithm accounts for the distribution of uncertainties and finds appropriate control actions even in the presence of large uncertainties. Such features allow safer and faster response to changes before the sufficient samples become available or before the parameter estimates converge. Moreover, it can be modularly added into an existing decision-making process: for example, it can be incorporated into the MPCs to balance between multiple objectives while ensuring chance-constrained conditions for nonlinear affine control systems without the assumption of Gaussian distributions. The resulting algorithms can properly control the long-term safe probabilities, which are defined based on future trajectories and intended control action, allowing that information to be used for producing more stable and safer action. Furthermore, the long-term safe probability can be learned continuously using past driving data, which in turn allows the control policy to be individually fine-tuned for an vehicle and its common driving conditions. By extending the outlook time horizon, preventive control actions can be executed before the system reaches a state where maintaining safety is no longer possible. Finally, the framework requires few assumptions in the choice of models: it can be adapted to different vehicle dynamics or tire models, ranging from white-box to gray-box to black-box models. The model also does not need to be differentiable—a common requirement when deterministic safe control algorithms that involve the computation of on (Lie) derivatives to be applied.

II. Algorithm Statement

In this section, we first introduce the generic vehicle model in section II-A, controller in section II-B, and the safety specifications in section II-C. Then, we present our proposed vehicle control algorithm in section II-D and performance guarantee in section II-E.

A. Vehicle Dynamics

We use $x \in \mathbb{R}^m$ to represent the state of the vehicle and $u \in \mathbb{R}^n$ to represent the control action. The dynamics of x depends on the physics and mechanics of the vehicle and the control action. We use

$$\dot{x} = F_x(x, \xi) + F_u(x)u, \tag{1}$$

with some possibly nonlinear functions F_x, F_u to represent the dynamics. The vehicle dynamics are parameterized by $\xi \in \mathbb{R}^l$. The values of ξ can change over time, so its exact values may not be accessible by the controller. The system dynamics in (1) is affine to the control action u. The proposed technique is agnostic to the choice of vehicle models, and thus F_x, F_u can be high-dimensional complex functions and/or built from data.

In order to implement the controller in digital systems, we discretize (1) as follows:

$$x_{k+1} = F(x_k, u_k, \xi_k), \tag{2}$$

where F is a function derived from (1). Here, Δt is the sampling time of the digital controller, and x_k and u_k are the value of x_t and u_t evaluated at the discrete time point $t = k\Delta t$, respectively.

B. Nominal controller

We assume the existence of an estimator for the vehicle parameters ξ. Let $\hat{\xi}_k$ denote the latest estimate of ξ available at time step k. The estimator may be operating in different time scale than the controller, in which case the estimate $\hat{\xi}$ could be updated intermittently. We additionally assume that the estimator also computes the confidence or posterior of the estimate. Let z denote the vehicle state and estimated parameter, *i.e.,*

$$z = \left[x^T,\ \hat{\xi}\right]^T \in \mathbb{R}^{m+l}. \tag{3}$$

The distribution of z_k is determined from the vehicle dynamics, estimator, and environmental changes.

The system is equipped a nominal MPC controller of the following form:

$$u_{k:k+H} = \underset{u_{k:k+H} \in \mathcal{U}}{\arg\min} \quad J(x_{k:k+H}, u_{k:k+H}) \tag{4a}$$

$$\text{s.t.} \quad C(x_{k:k+H}, u_{k:k+H}) \succeq 0 \tag{4b}$$

$$x_{i+1} = \hat{F}(x_i, u_i, \xi_i), i = k, \cdots, k+H \tag{4c}$$

where $x_{k:k+H} = \{x_k, x_{k+1}, \cdots, x_{k+H}\}$, and $u_{k:k+H} = \{u_k, u_{k+1}, \cdots, u_{k+H}\}$. Here, H is the MPC outlook horizon, and $\mathcal{U}$ is the optimization domain. In this optimization problem, the MPC cost function $J(x_k, u_k)$ for system state and control is minimized while satisfying the system dynamics (2). Condition (4b) are the MPC constraints, where $C(x_{k:k+H}, u_{k:k+H})$ is a vector valued function of $x_{k:k+H}, u_{k:k+H}$, and inequality (4b) is taken point-wise. The MPC uses system dynamics model (4c), which either equals or approximates the original dynamics (2). This controller is designed based on the performance specifications of the system and does not necessarily account for the safety specifications, described in the next subsection.

C. Safety specifications

We represent the safe event using set $\mathcal{S}$, which involves the internal state of the vehicle x and external/environmental variables. The safety specifications is then given by the following condition: the vehicle state stays within the safe set, *i.e.,*

$$x \in \mathcal{S}(\xi). \tag{5}$$

We assume this set is defined as the 0-superlevel set of a function $\phi : \mathbb{R}^m \times \mathbb{R}^l \to \mathbb{R}$, *i.e.,*

$$\mathcal{S}(\xi) = \{x : \phi(x, \xi) \geq 0\}. \tag{6}$$

A major challenge to ensure (5) arises from the uncertainties in the system. For example, safety depends on ξ, and when

it changes, the controller must adapt its action before an accurate estimate of ξ can be constructed from samples. When the uncertainty of ξ is large, it can be impossible to have (5) with probability 1. Moreover, ensuring (5) for all possible worst cases may not be feasible and/or leads to extreme control actions, which compromise the robustness and performance of the system. Instead, we aim to control the safe probability or recovery speed, formally defined below.

Safe probability. We want to ensure $x \in \mathcal{S}(\xi)$ during an outlook time window $\mathcal{T}(k) = \{k, k+1, \cdots, k+T\}$ with probability $1-\epsilon$: *i.e.,* , at any time $k \in \mathbb{Z}_+$,

$$\mathbb{P}(\exists \tau \in \mathcal{T}(k) \text{ s.t. } x_\tau \notin \mathcal{S}(\xi_\tau)) \leq \epsilon. \tag{7}$$

The outlook time horizon T should be sufficiently long to avoid myopic behaviors that are unsafe.

Recovery speed. We want to ensure the speed of recovery when condition (7) is violated. To formally state this condition, we first define a couple of notations. Let $\Psi(z)$ be the probability of the vehicle originating from state $z_k = z$ at time k to remain safe during outlook time horizon $\mathcal{T}(k)$, *i.e.,*

$$\Psi(z) := \mathbb{P}(x_\tau \in \mathcal{S}(\xi_\tau), \forall \tau \in \mathcal{T}(k) | z_k = z). \tag{8}$$

Note that, conditioned on $z_k = z$, this probability does not depend on k.[1] Let A denote the following discrete-time generator.

Definition 1 (Discrete-time Generator)**.** The discrete-time generator A of a discrete-time stochastic process $\{y_k \in \mathbb{R}^n\}_{k\in\mathbb{Z}_+}$ with sampling interval Δt evaluated at time k is given by

$$AG(y_k) = \frac{\mathbb{E}[G(y_{k+1})|y_k] - G(y_k)}{\Delta t} \tag{9}$$

whose domain is the set of all functions $G : \mathbb{R}^n \to \mathbb{R}$ of the stochastic process.

The discrete-time generator can be considered as the discrete-time counterpart of the infinitesimal generator for a continuous-time process. Using the above notations, the recovery condition can be formally stated as follows: when $\Psi(z_k) < (1-\epsilon)$,

$$\mathbb{E}\left[\frac{\Psi(z_{k+1}) - \Psi(z_k)}{\Delta t} | z_k\right] \geq \zeta(\Psi(z_k) - (1-\epsilon)). \tag{10}$$

Here, the function $\zeta : \mathbb{R}_- \to \mathbb{R}_+$ determines minimum recovery rate when the safety condition is violated by amount $\Psi(z_k) - (1-\epsilon)$. The risk tolerance level $\epsilon \in [0,1]$ and the recovery rate function ζ should be chosen to balance safe probability vs. nominal performance as well as the possibility of finding a feasible control action for the two objectives.

D. Proposed Control Algorithm

In this subsection, we propose an adaptive safe control method that exploits prediction and mediates behaviors based on the level of uncertainties. We first derive a sufficient condition that ensures safe probability based on a novel probabilistic forward invariance condition. The key novelty of this condition is that it can ensure long-term safety probability to be ensured using a myopic controller that can be computed in real-time onboard computation. The long-term safety probability can be computed offline and be continuously learned using the driving history. The controller only needs to myopically evaluate the immediate control action using a linear constraint, which can be easily integrated into optimization-based planning and control processes (*e.g.,* MPC [8]–[12]).

Specifically, we propose to constrain the control action u_k to satisfy the following conditions at all time $k \in \mathbb{Z}_+$:

$$A\Psi(z_k) \geq -\gamma(\Psi(z_k) - (1-\epsilon)). \tag{11}$$

Here, $\gamma : \mathbb{R} \to \mathbb{R}$ is a function that satisfies the following 4 design requirements:

Requirement 1: $\gamma(q)$ is strictly concave or linear in q.
Requirement 2: $\gamma(q) \leq q$ for any $q \geq 0$.
Requirement 3: $-\gamma(q) \geq \zeta(q)$ for any $q < 0$.

Condition (11) with design requirements 1 and 2 guarantees the safe probability condition (7) to hold. This condition is formally stated in theorem 1 in section II-E. Condition (11) with design requirements 1 and 3 ensures the recovery condition (10) to hold. This capability is formally stated in corollary 1.

Next, we show that $A\Psi(z_k)$ can be represented using a linear function of u_k when the sampling interval Δ is sufficiently small. Let $D(z)$ denote the first m entries of the gradient of $\Psi(z)$ evaluated at z, *i.e.,*

$$D(z) = [D^{(1)}(z), D^{(2)}(z), \cdots, D^{(m)}(z)]^T \in \mathbb{R}^m, \tag{12}$$

where

$$D^{(i)}(z) = \frac{\Psi(z^{(i)} + \Delta^{(i)}) - \Psi(z^{(i)} - \Delta^{(i)})}{2\Delta^{(i)}}. \tag{13}$$

Here, $\Delta^{(i)}$ denotes a vector that takes a scalar value of Δ in i-th entry and 0 otherwise. The scalar Δ is the step size to calculate the finite difference of the safe probability. Note that $D(z)$ has the same dimension with the state x. We make the following assumptions:

$$\lim_{\Delta t \to 0} \mathbb{E}\left[\frac{z_{k+1} - z_k}{\Delta t}\right] = \begin{bmatrix} F_x(x_k, u_k, \hat{\xi}_k) + F_u(x_k)u_k \\ 0 \end{bmatrix} \tag{14}$$

$$\lim_{\Delta t \to 0} \frac{1}{2\Delta t} \mathbb{E}\left[(z_{k+1} - z_k)^T M (z_{k+1} - z_k) \mid z_k\right] = c_k \tag{15}$$

$$\lim_{\Delta t \to 0} \frac{1}{\Delta t} \mathbb{E}\left[R_2(z_k, z_{k+1}) \mid z_k\right] = 0. \tag{16}$$

It is assumed in (14) that information about the future value of $\hat{\xi}$ is not available. In (15), c_k is a constant value and M is any matrix of appropriate dimension. Note that this term does not necessarily vanish (*e.g.,* Ito's calculus), but it will not depend on u. (16) implies that terms higher than third order vanish.

[1]This property holds because the system dynamics in (2) is time-invariant. The functions F_x and F_u do not depend on time.

Lemma 1. *Assume* (14)–(16) *hold. Then, the following condition holds.*

$$\lim_{\Delta t \to 0} A\Psi(z_k) = D(z_k) \cdot (F_x(x_k, \hat{\xi}_k) + F_u(x_k)u_k + c_k). \tag{17}$$

Proof (lemma 1) See extended version of this paper [13].

From Lemma 1, we can use sufficiently small sampling interval Δt and evaluate condition (11) using

$$D(z_k) \cdot (F_x(x_k, \hat{\xi}_k) + F_u(x_k)u + c_k) \geq -\gamma(\Psi(z_k) - (1-\epsilon)). \tag{18}$$

Condition (18) is a linear constraint, which can be used in LQ or convex problem without losing convexity. Therefore, it can be easily integrated into existing optimization-based controllers (*e.g.,* [14]–[17]) without much extra computational [8], [18]. For example, we can integrate the safe condition (18) with MPC as follows:

$$u_{k:k+H} = \underset{u_{k:k+H} \in \mathcal{U}}{\arg\min} \quad J(x_{k:k+H}, u_{k:k+H}), \tag{19a}$$

$$\text{s.t.} \quad C(x_{k:k+H}, u_{k:k+H}) \succeq 0, \tag{19b}$$

$$(2) \text{ and } (18). \tag{19c}$$

Here, the proposed condition (18) is imposed as an addition constraints in the nominal MPC controller (4).

The overall safe control strategy is given by Algorithm 1. At each time step k, Algorithm 1 functions as follows. In line 5, it obtains from the estimator the latest estimate $\hat{\xi}_k$ for the system parameter ξ. In line 6, it evaluates the functions Ψ and D at z_k either using online or offline computation. In an online setting, these values can be obtain by sampling the system dynamics (1) or (2). In an offline setting, these functions can be continuously learned from the past driving data. In line 7, it finds an control action u_k either using the optimization problem (19). This control action u_k is executed in line 8, and its impact on x_{k+1} is observed in line 4 at the next time step.

Algorithm 1 Safe control algorithm

1: Initialize Δz
2: $k \leftarrow 0$
3: **while** $k < K_{max}$ **do**
4: Observe x_k
5: Obtain $\hat{\xi}_k$ from the estimator
6: Obtain $\Psi(z_k)$ and $D(z_k)$ through Monte Carlo
7: Find $u_k \leftarrow$ **solve** $\{u_k$ in (19)$\}$
8: Execute action u_k
9: $k \leftarrow k + 1$
10: **end while**

E. Performance Guarantee

Theorem 1. *Consider the closed-loop system of* (2) *and* (4). *If system* (2) *originates at* $z_0 = z$ *with* $\Psi(z) > 1 - \epsilon$, *and the control action satisfies* (11) *with design requirements 1 and 2 at all time, then the following condition holds:*[2]

$$\mathbb{E}\left[\Psi(z_k)\right] \geq 1 - \epsilon \tag{20}$$

for all time $k \in \mathbb{Z}_+$.

Proof (theorem 1) See extended version of this paper [13].

Corollary 1. *Consider the closed-loop system of* (2) *and* (4) *where the control action satisfies* (11) *with design requirements 1 and 3 at all time. If* $\Psi(z_k) < 1 - \epsilon$ *at any time* $k \in \mathbb{Z}_+$, *then the recovery rate of the system is bounded from below by* (10).

Proof (corollary 1) See extended version of this paper [13].

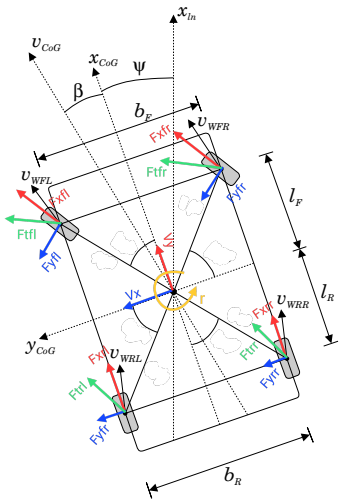

Fig. 1: Freebody diagram of the vehicle.

III. Experiment

We evaluated the efficacy of the proposed safe control method with simulation on a four-wheel 3-DoF vehicle. The design goal is to track a reference path without slipping. We present the vehicle dynamics in section III-A, the controller and the design specification in section III-B, and the results and discussions in section III-C.

A. Vehicle Model

We consider the vehicle model presented in [19] and Burckhardt's tire model based on the Kamm friction circle [20]. Fig. 1 shows the diagram of the vehicle model. In this model, each tire is associated with a longitudinal and lateral force. We use F_t to denote the total tire force on each of the four wheels, calculated as the squared sum of the lateral and longitudinal tire force. The saturated tire grip force is given by

$$F_{\text{sat}} = \mu m g / 4, \tag{21}$$

where m is the vehicle mass, and g is gravitational acceleration constant, μ is the friction coefficient between the tire

[2]Here, the expectation is taken over z_k conditioned on $z_0 = x$, and Ψ in (8) gives the probability of safety of the future trajectories $\{z_\kappa\}_{\{k+1,k+2,\cdots,k+T\}}$ conditioned on z_k.

and road (referred to as c_1 in Burckhardt's tire model). The vehicle system's state and controls are

$$x = [x_{\text{CoG}},\, y_{\text{CoG}},\, \psi,\, v_x,\, v_y,\, r,\, \omega_{fr},\, \omega_{fr},\, \omega_{rl},\, \omega_{rr},\, \delta]^T \tag{22}$$

$$u = \left[T_e,\ \dot{\delta}\right]^T, \tag{23}$$

where x_{CoG}, y_{CoG} and ψ are the vehicle inertial pose, v_x and v_y are vehicle frame velocities, r is the yaw rate, ω_{fl}, ω_{fr}, ω_{rl} and ω_{rr} are tire angular rates, δ is the steering angle, T_e is the input torque from the differential and $\dot{\delta}$ is the steering rate. The specific choice of parameters for simulation are summarized in the extended version of this paper [13].

B. Controllers and Design Specifications

The performance specification is to track a reference trajectory. This can be achieved by a linear time-varying MPC controller (LTV-MPC) of the form (4) with

$$\hat{F} = A_{\text{lin}}\, x_r + B_{\text{lin}}\, u_r, \tag{24a}$$

$$J = \frac{1}{2} x_e^T Q x_e + \frac{1}{2} u_e^T R u_e, \tag{24b}$$

$$C = L(X, Y), \tag{24c}$$

where A_{lin} and B_{lin} are the Jacobian of a reduced-order linearized vehicle dynamics, with states $x = [x_{\text{CoG}},\, y_{\text{CoG}},\, \psi,\, v_x,\, v_y,\, r]^T$ and controls $u = [\dot{v}_x,\, \delta]^T$ around a reference trajectory $[x_r, u_r]$ [21]. Reference trajectories are obtained from a B-spline based planner and reference generator demonstrated in [19]. The objective J is the weighted quadratic penalties on the trajectory tracking error $x_e = x - x_r$ and the difference between the actual control and the reference control $u_e = u - u_r$. Constraint function L is a linear time-varying function of the vehicle's position $[x_{\text{CoG}}, y_{\text{CoG}}]^T$, which characterizes the vehicle's distance to the lane boundaries around [21]. The constraint C limit the vehicle around the center of the lane. LTV-MPC linearizes the system at each time step, and predicatively optimize the control input in a given horizon H to make sure the vehicle is tracking the reference trajectory while satisfying necessary constraints.

The safety specification is to limit each tire's total force within a certain percentage $\eta \in (0, 1)$ of the maximum tire force F_{sat}, beyond which the vehicle starts to slip. The safety condition is defined by (6) with

$$\phi(x, \xi) = \min\Bigg\{1 - \left(\frac{4F_{tfl}}{\eta \xi m g}\right)^2, 1 - \left(\frac{4F_{tfr}}{\eta \xi m g}\right)^2, \\ 1 - \left(\frac{4F_{trl}}{\eta \xi m g}\right)^2, 1 - \left(\frac{4F_{trr}}{\eta \xi m g}\right)^2\Bigg\}, \tag{25}$$

where ξ is the estimation of the friction coefficient μ. With this definition, if any of the four tire's total force F_t exceed ηF_{sat}, then function $\phi(x, \xi)$ in (25) will become negative indicating that safety is being compromised. Accordingly, the proposed controller is given by (19) whose parameters are defined by (24). This controller essentially add to LTV-MPC a linear constraint (18) that ensures the long-term safe probability and probabilistic recovery speed.

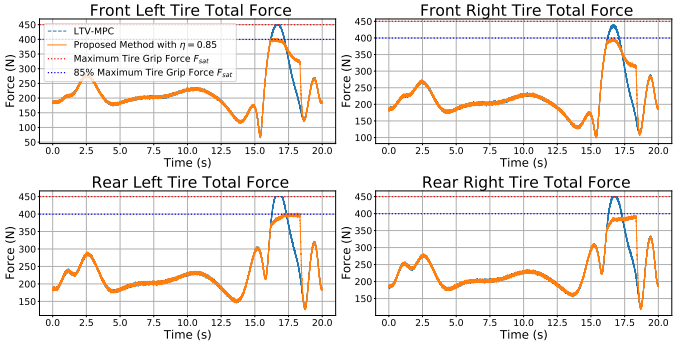

Fig. 2: Total tire force of each wheel.

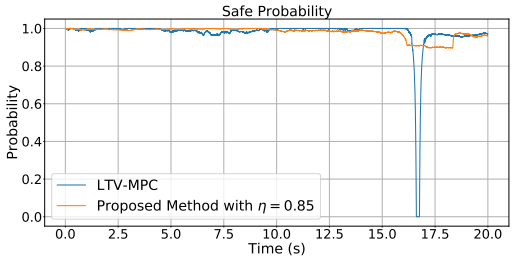

Fig. 3: The expected safe probability of the vehicle system.

C. Results

Fig. 2 shows the front and rear total tire force of the vehicle system as time evolves. With the proposed method, the tire force always stayed within the specified limit (85% of its saturation) with high probability. With LTV-MPC, the total tire force exceeded the maximum desired saturation rate after 15 seconds. Fig. 3 shows the safe probability Ψ in (8) with outlook horizon $T = 0.5$s with different controllers over time. With the proposed safe controller, the safe probability will not go below the desired percentage (90%, $\epsilon = 0.1$). This is consistent with the theoretical guarantee given in Theorem 1. This can be achieved because the proposed controller will look into the future and impose a more effective safe control on the system once the safe probability has an tendency of dropping, i.e., the system state is getting close to some potentially unsafe regions. In contrast, when LTV-MPC is used, the safe probability dropped significantly around 17s as the system approached undesired state regions. This is because LTV-MPC, which takes a deterministic framework, cannot constrain $x \in S(\xi)$ when the uncertainty of ξ is large. The contrasting behaviors suggest the importance of accounting for uncertainties.

Fig. 4 shows the reference trajectory and the actual trajectory of the vehicle under different controllers. The reference trajectory is designed to cut the road boundary during the cornering. Maximally tracking this reference trajectory with the reference speed will end up with getting out of the lane and losing traction. The LTV-MPC controller can maintain the vehicle in lane before the corner, but the vehicle started to slip during the cornering (see Fig. 2 during 15-18s) and could not track the reference well afterwards. With the proposed controller, the vehicle passed the corner without hitting the

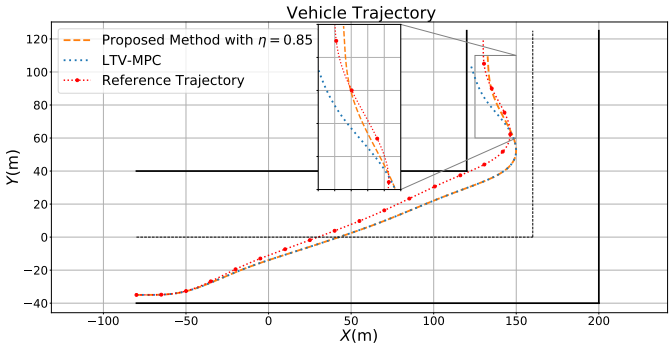

Fig. 4: Trajectory of the vehicle.

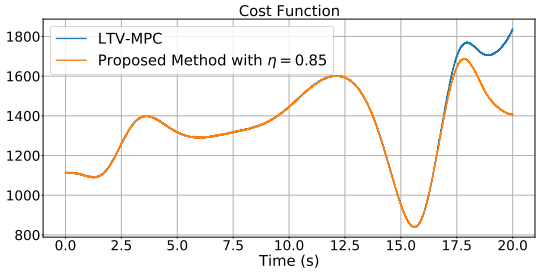

Fig. 5: The cost function values.

boundary nor losing traction. The performance of the two controllers is quantitatively characterized by the cost function value, which is shown in Fig. 5. The cost function of LTV-MPC is notably large after 17s, as the vehicle started to slip and deviated from the reference trajectory. On the other hand, the cost function of the proposed controller starts to decrease after 18s, indicating that the vehicle was under proper control and tracked the reference well after taking the corner. The results show that by imposing long-term safety constraints, our controller guarantees safety and, as a result, improves the performance of trajectory tracking, particularly in extreme driving with large uncertainties.

IV. Conclusion

In this paper, we propose a stochastic safe control technique for extreme driving conditions which can exploit prediction, mediate behaviors based on uncertainty, and adapt to changes. Through theoretical and numerical studies, we demonstrate its reliability, efficiency, and modularity. The reliability is due to its provable guarantee of long-term safe probability or probabilistic recovery speeds. The computational efficiency is achieved by imposing chance constraints for nonlinear systems and with non-Gaussian distributions by linear constraints online using offline computation. Finally, the derived safety condition can be modularly integrated into existing controllers, which largely improves its applicability.

References

[1] Q. Lu, A. Sorniotti, P. Gruber, J. Theunissen, and J. De Smet, "H loop shaping for the torque-vectoring control of electric vehicles: Theoretical design and experimental assessment," *Mechatronics*, vol. 35, pp. 32–43, 2016.

[2] L. Zhang, H. Ding, J. Shi, Y. Huang, H. Chen, K. Guo, and Q. Li, "An adaptive backstepping sliding mode controller to improve vehicle maneuverability and stability via torque vectoring control," *IEEE Transactions on Vehicular Technology*, vol. 69, no. 3, pp. 2598–2612, 2020.

[3] A. Parra, A. Zubizarreta, J. Pérez, and M. Dendaluce, "Intelligent torque vectoring approach for electric vehicles with per-wheel motors," *Complexity*, vol. 2018, 2018.

[4] A. D. Ames, J. W. Grizzle, and P. Tabuada, "Control barrier function based quadratic programs with application to adaptive cruise control," in *53rd IEEE Conference on Decision and Control*. IEEE, 2014, pp. 6271–6278.

[5] M. Wielitzka, M. Dagen, and T. Ortmaier, "Sensitivity-based road friction estimation in vehicle dynamics using the unscented kalman filter," in *2018 Annual American Control Conference (ACC)*. IEEE, 2018, pp. 2593–2598.

[6] L. Guo, H. Xu, J. Zou, H. Jie, and G. Zheng, "Variable gain control-based acceleration slip regulation control algorithm for four-wheel independent drive electric vehicle," *Transactions of the Institute of Measurement and Control*, vol. 43, no. 4, pp. 902–914, 2021.

[7] J. Zhou, H. Yue, J. Zhang, and H. Wang, "Iterative learning double closed-loop structure for modeling and controller design of output stochastic distribution control systems," *IEEE Transactions on Control Systems Technology*, vol. 22, no. 6, pp. 2261–2276, 2014.

[8] G. Bai, Y. Meng, L. Liu, W. Luo, and Q. Gu, "Review and comparison of path tracking based on model predictive control," *Electronics*, vol. 8, no. 10, p. 1077, 2019.

[9] F. Borrelli, A. Bemporad, M. Fodor, and D. Hrovat, "An mpc/hybrid system approach to traction control," *IEEE Transactions on Control Systems Technology*, vol. 14, no. 3, pp. 541–552, 2006.

[10] P. Falcone, F. Borrelli, J. Asgari, H. E. Tseng, and D. Hrovat, "Predictive active steering control for autonomous vehicle systems," *IEEE Transactions on control systems technology*, vol. 15, no. 3, pp. 566–580, 2007.

[11] T. Brüdigam, M. Olbrich, D. Wollherr, and M. Leibold, "Stochastic model predictive control with a safety guarantee for automated driving," *IEEE Transactions on Intelligent Vehicles*, pp. 1–1, 2021.

[12] A. Carvalho, Y. Gao, S. Lefevre, and F. Borrelli, "Stochastic predictive control of autonomous vehicles in uncertain environments," in *12th International Symposium on Advanced Vehicle Control*, 2014, pp. 712–719.

[13] S. Gangadhar, Z. Wang, H. Jing, and Y. Nakahira, "Dealing with Stochastic Uncertainty and Prediction in Extreme Driving," https://github.com/haomingj/Dealing-with-Stochastic-Uncertainty-and-Prediction-in-Extreme-Driving.

[14] P. Falcone, H. Eric Tseng, F. Borrelli, J. Asgari, and D. Hrovat, "Mpc-based yaw and lateral stabilisation via active front steering and braking," *Vehicle System Dynamics*, vol. 46, no. S1, pp. 611–628, 2008.

[15] H. Zhao, B. Ren, H. Chen, and W. Deng, "Model predictive control allocation for stability improvement of four-wheel drive electric vehicles in critical driving condition," *IET Control Theory & Applications*, vol. 9, no. 18, pp. 2688–2696, 2015.

[16] E. Siampis, E. Velenis, S. Gariuolo, and S. Longo, "A real-time nonlinear model predictive control strategy for stabilization of an electric vehicle at the limits of handling," *IEEE Transactions on Control Systems Technology*, vol. 26, no. 6, pp. 1982–1994, 2017.

[17] J. Yoon, W. Cho, J. Kang, B. Koo, and K. Yi, "Design and evaluation of a unified chassis control system for rollover prevention and vehicle stability improvement on a virtual test track," *Control Engineering Practice*, vol. 18, no. 6, pp. 585–597, 2010.

[18] M. Ataei, A. Khajepour, and S. Jeon, "Model predictive control for integrated lateral stability, traction/braking control, and rollover prevention of electric vehicles," *Vehicle system dynamics*, vol. 58, no. 1, pp. 49–73, 2020.

[19] M. Isaksson Palmqvist, "Model predictive control for autonomous driving of a truck," 2016.

[20] U. Kiencke and L. Nielsen, "Automotive control systems: for engine, driveline, and vehicle," 2000.

[21] P. Falcone, M. Tufo, F. Borrelli, J. Asgari, and H. E. Tseng, "A linear time varying model predictive control approach to the integrated vehicle dynamics control problem in autonomous systems," in *2007 46th IEEE Conference on Decision and Control*. IEEE, 2007, pp. 2980–2985.

V. Appendix

A. Proof

Proof (lemma 1). We want to show

$$\lim_{\Delta t\to 0} A\Psi(z_k) = D(z_k)\cdot(F_x(x_k,\hat{\xi}_k)+F_u(x_k)u_k+c_k). \quad (26)$$

Given a deterministic function $\Psi(z)$, from Taylor expansion,

$$\begin{aligned}\Psi(z_{k+1}) = \Psi(z_k) &+ (z_{k+1}-z_k)D\Psi(z_k)\\ &+ \frac{1}{2}(z_{k+1}-z_k)^T H\Psi(z_k)(z_{k+1}-z_k)\\ &+ R_2(z_k, z_{k+1}),\end{aligned} \quad (27)$$

where $R_2(z_k, z_{k+1}) = O\left(\|z_{k+1}-z_k\|^2\right)$, and $\lim_{z_{k+1}\to z_k} \frac{R_2(z_k,z_{k+1})}{\|z_{k+1}-z_k\|^2} = 0$. Then we have

$$\begin{aligned}&A\Psi(z_k)\\ &= \mathbb{E}\left[\frac{\Psi(z_{k+1})-\Psi(z_k)}{\Delta t} \mid z_k\right]\\ &= \mathbb{E}[\frac{1}{\Delta t}\{D\Psi(z_k)\cdot(z_{k+1}-z_k)\\ &\quad + \frac{1}{2}(z_{k+1}-z_k)^T D^2(z_k)(z_{k+1}-z_k)\\ &\quad + R_2(z_k,z_{k+1})\} \mid z_k]\\ &= D\Psi(z_k)\cdot\mathbb{E}\left[\frac{1}{\Delta t}(z_{k+1}-z_k) \mid z_k\right]\\ &\quad + \frac{1}{2\Delta t}\mathbb{E}\left[(z_{k+1}-z_t)^T M(z_{k+1}-z_k)|z_k\right]\\ &\quad + \frac{1}{\Delta t}\mathbb{E}\left[R_2(z_k,z_{k+1}) \mid z_k\right].\end{aligned} \quad (28)$$

■

Proof (theorem 1). We use mathematical induction to prove (20). Condition (20) holds for $k=0$ due to the assumption on initial condition. Next, we suppose (20) holds at time $k>0$, and show (20) holds for time $k+1$. Let

$$\mathbb{E}\left[\Psi(z_k)\right] = 1-\epsilon+q \quad (29)$$

for some $q \geq 0$. We first define the set of events H_i and variables $v_i, q_i,$ and δ_i, $i\in\{0,1\}$, as follows:

$$H_0 = \{\Psi(z_k) < 1-\epsilon\}, \quad (30)$$
$$H_1 = \{\Psi(z_k) \geq 1-\epsilon\}, \quad (31)$$
$$v_0 = \mathbb{E}\left[\Psi(z_k) \mid H_0\right] = 1-\epsilon-\delta_0, \quad (32)$$
$$v_1 = \mathbb{E}\left[\Psi(z_k) \mid H_1\right] = 1-\epsilon+\delta_1, \quad (33)$$
$$q_0 = \mathbb{P}(H_0), \quad (34)$$
$$q_1 = \mathbb{P}(H_1). \quad (35)$$

The left hand side of (29) can then be written as

$$\begin{aligned}\mathbb{E}[\Psi(z_k)] &= \mathbb{E}\left[\Psi(z_k) \mid H_0\right]\mathbb{P}(H_0) + \mathbb{E}\left[\Psi(z_k) \mid H_1\right]\mathbb{P}(H_1)\\ &= v_0q_0 + v_1q_1.\end{aligned} \quad (36)$$

From

$$\begin{aligned}\mathbb{E}\left[\Psi(z_k) \mid H_0\right] &< 1-\epsilon,\\ \mathbb{E}\left[\Psi(z_k) \mid H_1\right] &\geq 1-\epsilon,\end{aligned} \quad (37)$$

we obtain

$$\delta_0 \geq 0 \quad \text{and} \quad \delta_1 \geq 0. \quad (38)$$

Moreover, $\{q_i\}_{i\in\{0,1\}}$ satisfies

$$\mathbb{P}(H_0) + \mathbb{P}(H_1) = q_0 + q_1 = 1. \quad (39)$$

Combining (29) and (36) gives

$$1-\epsilon+q = v_0q_0 + v_1q_1. \quad (40)$$

Applying (32) and (33) to (40) gives

$$1-\epsilon+q = (1-\epsilon-\delta_0)\,q_0 + (1-\epsilon+\delta_1)\,q_1, \quad (41)$$

which, combined with (39), yields

$$q = \delta_1q_1 - \delta_0q_0. \quad (42)$$

On the other hand, we have

$$\begin{aligned}&\mathbb{E}\left[\gamma\left(\Psi(z_k)-(1-\epsilon)\right)\right] && (43)\\ &\quad= \mathbb{P}(H_0)\left(\mathbb{E}\left[\gamma\left(\Psi(z_k)-(1-\epsilon)\right) \mid H_0\right]\right)\\ &\qquad+ \mathbb{P}(H_1)\left(\mathbb{E}\left[\gamma\left(\Psi(z_k)-(1-\epsilon)\right) \mid H_1\right]\right) && (44)\\ &\quad= q_0\left(\mathbb{E}\left[\gamma\left(\Psi(z_k)-(1-\epsilon)\right) \mid H_0\right]\right)\\ &\qquad+ q_1\left(\mathbb{E}\left[\gamma\left(\Psi(z_k)-(1-\epsilon)\right) \mid H_1\right]\right) && (45)\\ &\quad\leq q_0\left(\gamma\left(\mathbb{E}\left[\Psi(z_k)-(1-\epsilon) \mid H_0\right]\right)\right)\\ &\qquad+ q_1\left(\gamma\left(\mathbb{E}\left[\Psi(z_k)-(1-\epsilon) \mid H_1\right]\right)\right) && (46)\\ &\quad= q_0\left(\gamma\left(-\delta_0\right)\right) + q_1\left(\gamma\left(\delta_1\right)\right) && (47)\\ &\quad\leq \gamma\left(-q_0\delta_0 + q_1\delta_1\right) && (48)\\ &\quad= \gamma(q) && (49)\\ &\quad\leq q. && (50)\end{aligned}$$

Here, (45) is due to (34) and (35); (46) is obtained from Jensen's inequality for concave function γ; (47) is based on (32) and (33); (48) is due to Jensen's inequality, design requirement 1 and (39); and (49) is due to (42). From (43) to (50), we have

$$\mathbb{E}\left[-\gamma\left(\Psi(z_k)-(1-\epsilon)\right)\right] \geq -q. \quad (51)$$

Recall that the control action is chosen to satisfy (11). Now, we take the expectation over both side of (11) to obtain

$$\mathbb{E}[A\Psi(z_k)] \geq \mathbb{E}[-\gamma(\Psi(z_k)-(1-\epsilon))]. \quad (52)$$

From (9), we have

$$A\Psi(z_k) = \frac{\mathbb{E}[\Psi(z_{k+1})-\Psi(z_k)|z_k]}{\Delta t}. \quad (53)$$

Therefore, (52) can be written as

$$\frac{\mathbb{E}[\mathbb{E}[\Psi(z_{k+1})-\Psi(z_k)|z_k]]}{\Delta t} \geq \mathbb{E}[-\gamma(\Psi(z_k)-(1-\epsilon))]. \quad (54)$$

Using the law of total expectation, we have

$$\frac{\mathbb{E}[\Psi(z_{k+1})-\Psi(z_k)]}{\Delta t} \geq \mathbb{E}[-\gamma(\Psi(z_k)-(1-\epsilon))]. \quad (55)$$

Combining (29), (51), (55) and design requirement 2 yields

$$\mathbb{E}[\Psi(z_{k+1})] \geq \mathbb{E}[\Psi(z_k)] + \mathbb{E}[-\gamma(\Psi(z_k) - (1-\epsilon))]\Delta t \tag{56}$$

$$\geq 1 - \epsilon + q - q\Delta t \tag{57}$$

$$= 1 - \epsilon + q(1 - \Delta t). \tag{58}$$

Since $\Delta t \ll 1$ and $q \geq 0$, we have

$$\mathbb{E}[\Psi(z_{k+1})] \geq 1 - \epsilon. \tag{59}$$

■

Proof (corollary 1). Let

$$\Psi(z_k) = 1 - \epsilon + q \tag{60}$$

for some $q < 0$. We have

$$\frac{1}{\Delta t}(\mathbb{E}[\Psi(z_{k+1})] - \Psi(z_k)) \tag{61}$$

$$= A\Psi(z_k) \tag{62}$$

$$\geq -\gamma(\Psi(z_k) - (1-\epsilon)) \tag{63}$$

$$\geq \zeta(q), \tag{64}$$

where (62) holds from definition 1, (63) is due to (11), and (64) is due to design requirement 3. From (61)–(64), we have

$$\frac{1}{\Delta t}\mathbb{E}[\Psi(z_{k+1}) - \Psi(z_k)] \geq \zeta(\Psi(z_k) - (1-\epsilon)). \tag{65}$$

■

B. Complete Vehicle Model

1) Ground point tire velocities: First, we compute the total ground point velocities at each tire due to the vehicle's motion. We assume a track width W and wheelbase $L = l_f + l_r$

$$v_{\text{W fl}} = v_{\text{CoG}} - r\left(\frac{W}{2}\cos\beta - l_f \sin\beta\right) \tag{66}$$

$$v_{\text{W fr}} = v_{\text{CoG}} + r\left(\frac{W}{2}\cos\beta + l_f \sin\beta\right) \tag{67}$$

$$v_{\text{W rl}} = v_{\text{CoG}} - r\left(\frac{W}{2}\cos\beta + l_r \sin\beta\right) \tag{68}$$

$$v_{\text{W rr}} = v_{\text{CoG}} + r\left(\frac{W}{2}\cos\beta - l_r \sin\beta\right) \tag{69}$$

Where, β is the angle between the velocity slip angle at the vehicle's CoG and is given as:

$$\beta = \frac{l_r}{L}\tan\delta \tag{70}$$

2) Tire Lateral Slip Angle: For computing the slip angle we assume a single-track steering angle δ for the front tires as such:

$$\tan(\delta - \alpha_{\text{fl}}) = \frac{l_f r + v_{\text{CoG}}\sin\beta}{v_{\text{CoG}}\sin\beta} \tag{71}$$

$$\tan(\delta - \alpha_{\text{fr}}) = \frac{l_f r + v_{\text{CoG}}\sin\beta}{v_{\text{CoG}}\sin\beta} \tag{72}$$

$$\tan\alpha_{\text{rl}} = \frac{l_r r - v_{\text{CoG}}\sin\beta}{v_{\text{CoG}}\sin\beta} \tag{73}$$

$$\tan\alpha_{\text{rr}} = \frac{l_r r - v_{\text{CoG}}\sin\beta}{v_{\text{CoG}}\sin\beta} \tag{74}$$

3) Longitudinal and Lateral Slip: For each tire, given the wheel's rotational velocity $v_{\text{R}} = R\omega$, the ground point velocity v_{W}, and lateral slip angle α, we calculate the longitudinal (s_L) and lateral (s_S) slip ratios as follows:

$$s_L = \frac{v_{\text{R}} - v_{\text{W}}}{\max\{v_{\text{W}}, v_{\text{R}}\cos\alpha\}} \tag{75}$$

$$s_S = \tan\alpha 1(s_L) + \frac{v_{\text{R}}}{v_{\text{W}}}\sin\alpha 1(-s_L) \tag{76}$$

$$s_{\text{Res}}^2 = s_L^2 + s_S^2 \tag{77}$$

Where $1(x)$ is the Heaviside step function. (78)

4) Tire Forces: Based on the each tire's longitudinal and tire slip calculations, we can calculate the longitudinal (F_{L}) and lateral (F_{S}) forces generated in the respective tire's frame of reference:

$$F_{\text{L rl}} = mg\frac{\mu(s_{\text{Res rl}})}{s_{\text{Res rl}}}(s_{\text{L rl}}\cos\alpha_{\text{rl}} + s_{\text{S rl}}\sin\alpha_{\text{rl}}) \tag{79}$$

$$F_{\text{S rl}} = mg\frac{\mu(s_{\text{Res rl}})}{s_{\text{Res rl}}}(-s_{\text{L rl}}\sin\alpha_{\text{rl}} + s_{\text{S rl}}\cos\alpha_{\text{rl}}) \tag{80}$$

$$F_{\text{L rr}} = mg\frac{\mu(s_{\text{Res rr}})}{s_{\text{Res rr}}}(s_{\text{L rr}}\cos\alpha_{\text{rr}} + s_{\text{S rr}}\sin\alpha_{\text{rr}}) \tag{81}$$

$$F_{\text{S rr}} = mg\frac{\mu(s_{\text{Res rl}})}{s_{\text{Res rr}}}(-s_{\text{L rr}}\sin\alpha_{\text{rr}} + s_{\text{S rr}}\cos\alpha_{\text{rr}}) \tag{82}$$

$$F_{\text{L fl}} = mg\frac{\mu(s_{\text{Res fl}})}{s_{\text{Res fl}}}(s_{\text{L fl}}\cos\alpha_{\text{fl}} + s_{\text{S fl}}\sin\alpha_{\text{fl}}) \tag{83}$$

$$F_{\text{S fl}} = mg\frac{\mu(s_{\text{Res fl}})}{s_{\text{Res fl}}}(-s_{\text{L fl}}\sin\alpha_{\text{fl}} + s_{\text{S fl}}\cos\alpha_{\text{fl}}) \tag{84}$$

$$F_{\text{L fr}} = mg\frac{\mu(s_{\text{Res fr}})}{s_{\text{Res fr}}}(s_{\text{L fr}}\cos\alpha_{\text{fr}} + s_{\text{S fr}}\sin\alpha_{\text{fr}}) \tag{85}$$

$$F_{\text{S fr}} = mg\frac{\mu(s_{\text{Res fr}})}{s_{\text{Res fr}}}(-s_{\text{L fr}}\sin\alpha_{\text{fr}} + s_{\text{S fr}}\cos\alpha_{\text{fr}}) \tag{86}$$

Then we convert the tire forces into the vehicle's frame as follows:

$$F_{\text{X fl}} = F_{\text{L fl}} \cos\delta - F_{\text{S fl}} \sin\delta \tag{87}$$
$$F_{\text{Y fl}} = F_{\text{S fl}} \cos\delta + F_{\text{L fl}} \sin\delta \tag{88}$$
$$F_{\text{X fr}} = F_{\text{L fr}} \cos\delta - F_{\text{S fr}} \sin\delta \tag{89}$$
$$F_{\text{Y fr}} = F_{\text{S fr}} \cos\delta + F_{\text{L fr}} \sin\delta \tag{90}$$
$$F_{\text{X rl}} = F_{\text{L rl}} \tag{91}$$
$$F_{\text{Y rl}} = F_{\text{S rl}} \tag{92}$$
$$F_{\text{X rr}} = F_{\text{L rr}} \tag{93}$$
$$F_{\text{Y rr}} = F_{\text{S rr}} \tag{94}$$

With this, we have obtained the Lateral and Longitudinal tire forces for each of the four vehicle's tires (rl, rr, fl, fr)

5) Drivetrain Model: We assume an open drivetrain with equal torque distribution and linear dynamics, as shown below:

$$J_\omega \dot{\omega}_{\text{fl}} = -aF_{\text{L fl}} + \frac{1}{4}T_e \tag{95}$$
$$J_\omega \dot{\omega}_{\text{fr}} = -aF_{\text{L fr}} + \frac{1}{4}T_e \tag{96}$$
$$J_\omega \dot{\omega}_{\text{rl}} = -aF_{\text{L rl}} + \frac{1}{4}T_e \tag{97}$$
$$J_\omega \dot{\omega}_{\text{rr}} = -aF_{\text{L rr}} + \frac{1}{4}T_e \tag{98}$$

Where, J_ω is the wheel inertia, a is the wheel radius, and τ_ω is the driving torque from the engine/motor.

6) Complete Vehicle Model: We can now write down the complete vehicle dynamics as follows:

$$\dot{x}_{\text{CoG}} = v_x \cos\psi - v_y \sin\psi \tag{99}$$
$$\dot{y}_{\text{CoG}} = v_x \sin\psi + v_y \cos\psi \tag{100}$$
$$\dot{\psi} = r \tag{101}$$
$$\begin{aligned} m\dot{v_x} = {} & mv_y r + F_{\text{X fl}} + \\ & F_{\text{X fr}} + F_{\text{X rl}} + F_{\text{X rr}} \end{aligned} \tag{102}$$
$$\begin{aligned} m\dot{v_y} = {} & -mv_y r + F_{\text{Y fl}} + \\ & F_{\text{Y fr}} + F_{\text{Y rl}} + F_{\text{Y rr}} \end{aligned} \tag{103}$$
$$\begin{aligned} I_z \dot{r} = {} & l_f \left(F_{\text{Y fl}} + F_{\text{Y fr}}\right) \\ & - l_r \left(F_{\text{Y rl}} + F_{\text{Y rr}}\right) \\ & + \frac{W}{2}\left(-F_{\text{X rl}} + F_{\text{X rr}}\right) \\ & + \frac{W}{2}\left(-F_{\text{X fl}} + F_{\text{X fr}}\right) \end{aligned} \tag{104}$$
$$J_\omega \dot{\omega}_{\text{fl}} = -aF_{\text{L fl}} + \frac{1}{4}T_e \tag{105}$$
$$J_\omega \dot{\omega}_{\text{fr}} = -aF_{\text{L fr}} + \frac{1}{4}T_e \tag{106}$$
$$J_\omega \dot{\omega}_{\text{rl}} = -aF_{\text{L rl}} + \frac{1}{4}T_e \tag{107}$$
$$J_\omega \dot{\omega}_{\text{rr}} = -aF_{\text{L rr}} + \frac{1}{4}T_e \tag{108}$$
$$\dot{\delta} = \dot{\delta} \tag{109}$$